

# The detection of the donor star in IY UMa

Daniel J. Rolfe<sup>1,2</sup>, Timothy M. C. Abbott<sup>3,4</sup> and Carole A. Haswell<sup>2</sup>

<sup>1</sup>*Department of Physics & Astronomy, University of Leicester, University Road, Leicester, LE1 7RH, UK.*

<sup>2</sup>*Department of Physics & Astronomy, The Open University, Walton Hall, Milton Keynes, MK7 6AA, UK.*

<sup>3</sup>*Cerro Tololo Inter-American Observatory, Casilla 603, La Serena, Chile*

<sup>4</sup>*Nordic Optical Telescope, Roque del Los Muchachos & Santa Cruz de La Palma, Canary Islands, Spain*

Accepted. Received

## ABSTRACT

We present the results of a search for the donor star in the high inclination SU UMa type cataclysmic variable IY UMa. We detect absorption features in the near infrared consistent with an M type dwarf donor star. Using the skew mapping technique to exploit the velocity information provided by the 8183–8194 Å Na I absorption doublet, we locate the absorption at the expected donor velocity of IY UMa.

**Key words:** stars: novae, cataclysmic variables, stars: individual: IY UMa, stars: dwarf novae, techniques: spectroscopic

## 1 INTRODUCTION

IY UMa is a dwarf nova cataclysmic variable (CV). Patterson et al. (2000) (hereafter P2000) and Rolfe, Haswell and Patterson (2001) present detailed photometric studies of the January 2000 superoutburst and superhump phenomenon. Spectroscopic observations have been published, revealing a bright hotspot and deep white dwarf absorption lines during quiescence (Rolfe, Abbott & Haswell 2001, Patterson et al. 2000, Rolfe et al. 2002); an eccentric disc during superoutburst (Wu et al. 2001); and lines powered by reprocessed boundary layer emission during outburst (Rolfe, Abbott & Haswell 2002 and Rolfe et al. 2002).

The orbital period of IY UMa is 1.77 hours, and Patterson et al. (2000) estimated  $M_{wd} = 0.86 \pm 0.11 M_{\odot}$ ,  $M_{donor} = 0.12 \pm 0.02 M_{\odot}$  and orbital inclination  $i = 86^{\circ}.8 \pm 1^{\circ}.5$ . Direct measurements of orbital parameters are desirable. A model-independent solution can be obtained if the orbital period and white dwarf eclipse width (already accurately measured for IY UMa) can be combined with measurements of the donor and white dwarf orbital velocities. The orbital period suggests a spectral type of M4.2 to M6.3 for the donor in IY UMa (Equation 4 in Smith & Dhillon (1998)). Thus absorption features in the far optical and near infrared are expected cf. Z Cha and HT Cas (Wade & Horne 1988 and Marsh 1990). We obtained spectroscopic observations of IY UMa to look for these absorption features in the wavelength range 7000–8300 Å.

## 2 OBSERVATIONS AND DATA REDUCTION

Observations were taken on 2001 Jan 3 and 4 using AL-FOSC on the Nordic Optical Telescope. A few calibration images were taken on Jan 7. A slit width of 1.2'' was used

**Table 1.** M dwarf template stars

Object	Spectral type	Reference
GJ 1154, Zkh 176	M5V	Zakhozhaj (1979)
GJ 228B, Zkh 84	M4V	Zakhozhaj (1979)
BD+28 2110	M3V	Ungren (1962)
CTI 092053.7+280101	M1.5V	Kirkpatrick et al. (1994)

with GRISM 8 yielding a FWHM resolution of  $\sim 6.2 \text{ \AA}$  and dispersion 1.24 Å per pixel. We discuss only the red end of the spectra here (7000–8350 Å). 39 360-second exposures of IY UMa and a nearby comparison were obtained, along with exposures of several M type dwarfs for use as template stars (listed in Table 1). Frequent arc lamp exposures provided wavelength calibration (giving  $9 \text{ km s}^{-1}$  r.m.s. velocity variation in the sky lines) while HD 93521 served as a flux standard and telluric standard.

Data reduction was carried out using IRAF. The CCD suffers from fringing but normalized lamp flats were used to flat-field the images and removed all detectable traces of the fringing pattern. The TELLURIC package in IRAF was used to correct for telluric features. Apart from the strongest feature around 7600 Å, the telluric correction worked quite well.

Conditions were not photometric so flux calibration of these red spectra was not possible. However, the skew mapping technique relies on normalized spectra. Each spectrum was normalized by fitting a 4th order polynomial to the continuum regions and dividing by this.

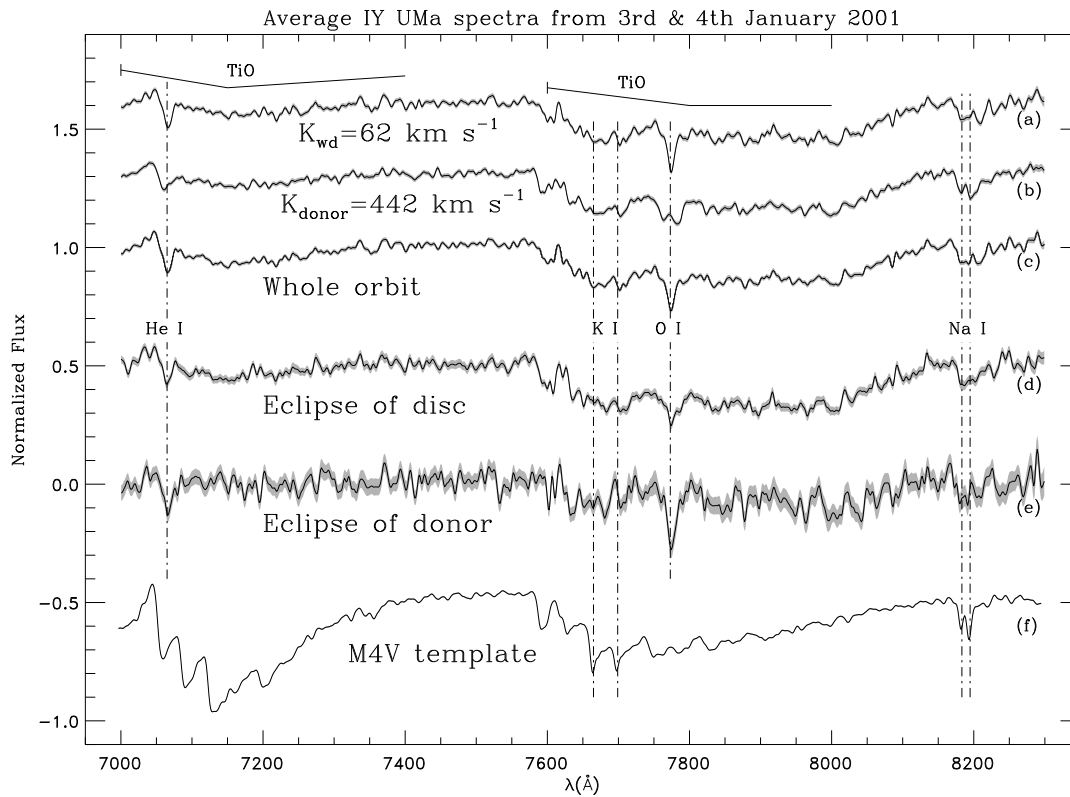


**Figure 1.** Average red spectra of IY UMa on 3rd & 4th January 2001. (a) shows average in rest frame of white dwarf, (b) in rest frame of donor, (c) in frame of observer. (d) shows average when donor eclipses disc and white dwarf, (e) when disc obscures donor. (f) shows M4V template spectrum. Shaded regions show error bars.

### 3 AVERAGE SPECTRA

Various different averages of the IY UMa spectra are shown in Figure 1a–e along with the M4V dwarf spectrum in Figure 1f. Each plotted spectrum has been Gaussian smoothed with FWHM of 4 pixels (less than the FWHM spectral resolution), and shifted in flux by a multiple of 0.5 units.

Figure 1c shows the average of all 39 IY UMa spectra. The most obvious features are the He I emission and core absorption at 7065Å, the 7773Å O I absorption, the broad absorption band around 7600Å to 8200Å and the absorption line around 8200Å. The He I is from the disc.

The broad 7600Å–8200Å feature matches the TiO absorption band seen in the M dwarf spectra, where it is strongest in the M5V dwarf. Figures 1d & 1e show average spectra of IY UMa during eclipse (orbital phases -0.1–0.1) and where the donor should be partially obscured by the disc (phase 0.42–0.58 assuming a quiescent disc radius of  $0.25a$  (Stanishev et al. 2001)). The TiO absorption is clearly much stronger (by a factor  $\sim 2$ ) when the donor eclipses the disc than when the disc obscures the donor, confirming the identification of this feature as the TiO band absorption in the donor.

The 7773Å O I triplet has been seen in many CVs. A study of 65 CVs by Friend et al. (1988) reveals this feature in absorption in several systems during outburst, but in emission during quiescence. HT Cas also shows this feature in emission during quiescence (Marsh 1990). Friend et al. (1988) attribute this to line emission from an optically thin disc in quiescence, and absorption from an optically thick

disc in outburst. Two high inclination systems, Z Cha (Wade & Horne 1988) and V2051 Oph (Friend et al. 1988), show a broad emission from the O I triplet, superimposed with a narrower absorption component. It is possible that a broad weak emission component is also present in these IY UMa spectra. Friend et al. (1988) suggest that the narrow absorption feature is absorption of white dwarf emission by the disc, something which we might expect in high inclination systems. That this feature arises from the disc and certainly not from the donor is confirmed by Figures 1a & b, where each individual spectrum was Doppler-shifted into the rest frame of the white dwarf or donor before adding together the spectra. The velocities of the donor and white dwarf were assumed to be  $K_2 = 442 \text{ km s}^{-1}$  and  $K_1 = 62 \text{ km s}^{-1}$  respectively, calculated using the P2000 orbital parameters. In the rest frame of the white dwarf the O I feature remains sharp, while in the donor star frame it splits into two absorption dips. In addition, the depth of this absorption is significantly stronger when the disc is in front of the donor (Figure 1e) than when the donor eclipses the disc (Figure 1d).

The 8200Å absorption feature closely matches the 8183–8194Å Na I doublet seen in all four dwarf template spectra. In the average spectrum (Figure 1c) it does not have the same doublet structure as seen in the template spectra, but when shifted to the donor rest frame (Figure 1b) the doublet structure becomes apparent, clearly matching the laboratory wavelengths. This feature is also more significant (considering the flux errors) during disc eclipse (Figure 1d) than when

the disc passes in front of the donor (Figure 1e). This is a clear detection of the Na I doublet, a feature which has been exploited to measure  $K_2$  in other CVs, c.f. Wade & Horne (1988), Friend et al. (1988, 1990a, 1990b) and Marsh (1990).

The TiO absorption band around 7000Å–7400Å is also more prominent when the donor obscures the disc than when the disc obscures the donor. The K I lines at 7665Å and 7699Å are not clearly seen, but there are weak features close to the noise level which could be tentatively identified as these lines.

Weaker Na I and TiO absorption around phase 0.5 than at other phases has been seen before in dwarf novae, e.g. Z Cha (Wade & Horne 1988), HT Cas (Marsh 1990) and SS Cyg (Hessman et al. 1984), and was attributed to a non-uniform distribution of absorption across the surface of the donor. The suggested cause of this non-uniform distribution is the filling-in of absorption features on the inner face of the donor by irradiation from the disc and/or white dwarf. This, rather than eclipse of the donor by the disc, might also be the cause of the weakened features around phase 0.5 in IY UMa.

The absorption feature at 7600Å is probably a combination of residual atmospheric absorption and the 7600Å feature seen in M dwarf spectra. There is some evidence of over-correction of the telluric absorption in the M5V template around 8230Å.

We see no evidence of Paschen emission around 8200Å seen in some CVs e.g. TT Ari and V603 Aql (Friend et al. 1988).

The donor star in IY UMa has been detected, showing all the expected features of a late M dwarf star. Without flux calibrated spectra, the relative strengths of the absorption features cannot be used to estimate more precisely the spectral type of the donor. The low signal-to-noise ratio prevents us from exploiting the Na I doublet to measure  $K_2$  directly from the spectra, so we adopt the skew mapping technique (Smith, Cameron & Tucknott 1993) to locate the donor in velocity space.

#### 4 SKEW MAPPING

Skew mapping is the best method for detecting the donor and determining its velocity when the absorption features are weak. This technique has been successfully employed for several systems (e.g. Smith, Cameron and Tucknott (1993), Smith, Dhillon and Marsh (1998) and recently in VY Aqr (Littlefair et al 2000)). Skew mapping co-adds spectra to increase signal-to-noise, while also correcting each spectrum for the orbital motion of the donor, to avoid smearing out donor absorption features. Skew mapping extends the technique used in producing Figure 1b (where  $K_2$  was assumed), by cross-correlating each such co-added spectrum with a template donor star spectrum, and finding the combination of template star and donor velocity at which the cross-correlation peak is strongest. This process is equivalent to producing a trailed “cross-correlation spectrum”, and then back-projecting this trail into velocity space, producing a cross-correlation map in velocity-space (the skew map) which should show a peak at the velocity of the donor star.

The normalized spectra of the template M dwarfs and

IY UMa were continuum subtracted, and were Gaussian smoothed with FWHM of 2.5 pixels to increase S/N without losing any spectral information. Each IY UMa spectrum,  $F(\lambda)$ , was cross correlated with the template spectrum,  $T(\lambda)$ , for a range of velocity shifts,  $v$ , using correlation coefficient  $C_v$  defined as

$$C_v = \frac{\sum_{\lambda=\lambda_{min}}^{\lambda_{max}} F(\lambda)T'_v(\lambda)}{\left(\sum_{\lambda=\lambda_{min}}^{\lambda_{max}} F(\lambda)^2 \sum_{\lambda=\lambda_{min}}^{\lambda_{max}} T'_v(\lambda)^2\right)^{\frac{1}{2}}}, \quad (1)$$

where  $T'_v(\lambda) = T\left(\frac{\lambda}{1+v/c}\right)$ . This definition of  $T'_v(\lambda)$  simply has the effect of red-shifting the template spectrum by velocity  $v$  before cross-correlating. The denominator of  $C_v$  is chosen so that if the template and donor spectra are identical, the value of  $C_v$  at the peak will be 1, independent of any simple scaling of the flux of either spectrum. The correlation trails thus produced were then transformed to velocity-space using the Fourier-filtered back-projection technique as implemented in Tom Marsh’s MOLLY software. The strength of the skew map at a given velocity therefore shows how well the object spectra match a star of the template’s spectral type orbiting at that velocity.

Only the Na I doublet wavelength range was used in the cross-correlation, since this is the only sharp donor absorption feature detected, and will therefore provide all the velocity information. Skew maps were also produced using the spectral range  $\lambda = 7045\text{--}8240\text{\AA}$  (with the O I and He I lines masked out) which uses all the detected donor star features, but this simply smears out the donor star in the skew map, probably a result of the broad TiO absorptions showing a strong correlation but low velocity sensitivity. The normalization of the spectrum around the Na I doublet was improved by fitting a straight line to the continuum either side of the doublet. The skew map also depends upon the relative systemic velocity of IY UMa and the template star. Neither of these is yet known, although measurements of H $\alpha$  emission lead to estimates for IY UMa of  $\gamma = 13.6 \pm 1 \text{ km s}^{-1}$  (Rolfe et al. 2002) and  $\gamma = -4 \pm 32 \text{ km s}^{-1}$  (Wu et al. 2001). Such estimates should be treated with caution, however, since the determination of systemic velocity from emission lines is notoriously unreliable: effects such as phase-dependent occultation/absorption of emission and temporal variations in emission can produce incorrect results. By cross-correlating the M3V template whose systemic velocity is  $1 \text{ km s}^{-1}$  (Evans 1967) with the other four templates, the systemic velocities of these stars were determined. The skew maps for each template were produced for a range of values of the IY UMa systemic velocity,  $\gamma_{IYUMa}$ , between -100 and  $300 \text{ km s}^{-1}$  (the low resolution of our spectra limits the accuracy of our systemic velocity determinations). This was identified as a suitable range for  $\gamma_{IYUMa}$  after initially studying the range  $-750\text{--}750 \text{ km s}^{-1}$ . This procedure enables a determination of the value which produces the clearest peak. We do not consider this a determination of the systemic velocity of IY UMa.

The orbital phase range 0.42 to 0.58 was not included when producing the back projections to avoid the weakened/obscured absorption lines around this phase interfering with the results. The results from using the entire phase range are considered at the end of this section.

Figure 2 shows a phase-folded and -binned and velocity-

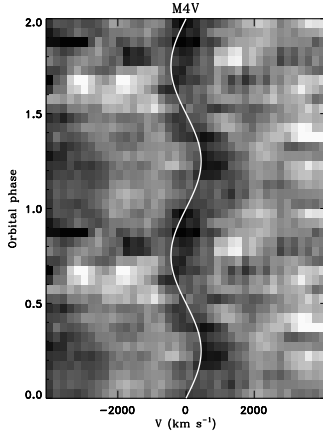


**Figure 2.** Cross-correlation trail for the M4V template

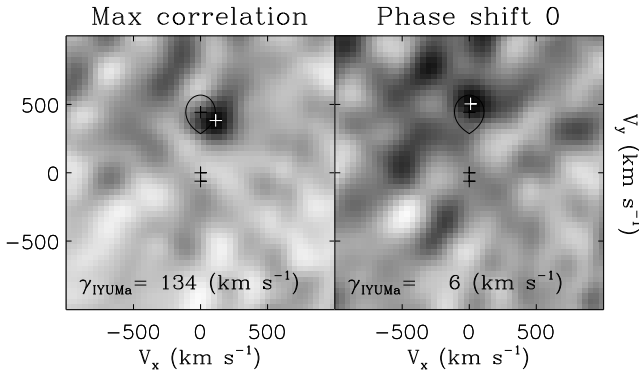


**Figure 3.** IY UMa skew maps using the M4V template. The teardrop shows the expected velocity of the donor, and the black crosses show the white dwarf, system and donor centre of mass velocities. The white cross is the measured peak maximum.

binned correlation trail for the M4V template. All four templates yield almost identical trails; at this low resolution and signal-to-noise, differences in structure in the NaI doublet between the spectral types are not going to be distinguishable in the IY UMa observations. The trail shows an S-wave, corresponding to a localized region in velocity space at which the IY UMa spectrum best matches the sodium feature. The peak-peak amplitude of this feature is about  $1000 \text{ km s}^{-1}$ , and is at minimum excursion around orbital phase 0. This phasing and amplitude is in agreement with the predicted orbital motion of the donor (plotted in white in Figure 2) using the P2000 orbital parameters (line-of-sight donor velocity semi-amplitude  $442 \text{ km s}^{-1}$ ). The velocities are heliocentric and corrected for the template systemic velocity.

The trails were transformed to velocity space. The resulting skew maps have a clear maximum close to the predicted location of the donor star using the P2000 parameters. The exact location of the maximum depends on the assumed IY UMa systemic velocity,  $\gamma_{\text{IYUMa}}$ . Two skew maps for the M4V template are shown in Figure 3. The map in the left panel uses the value of  $\gamma_{\text{IYUMa}}$  which produces the strongest peak (i.e. max correlation), while that on the right corresponds to the  $\gamma_{\text{IYUMa}}$  which produces a peak with no x-component of velocity (as expected for the donor). These values of  $\gamma_{\text{IYUMa}}$  were determined as described below.

The velocity and width of the peak was determined for

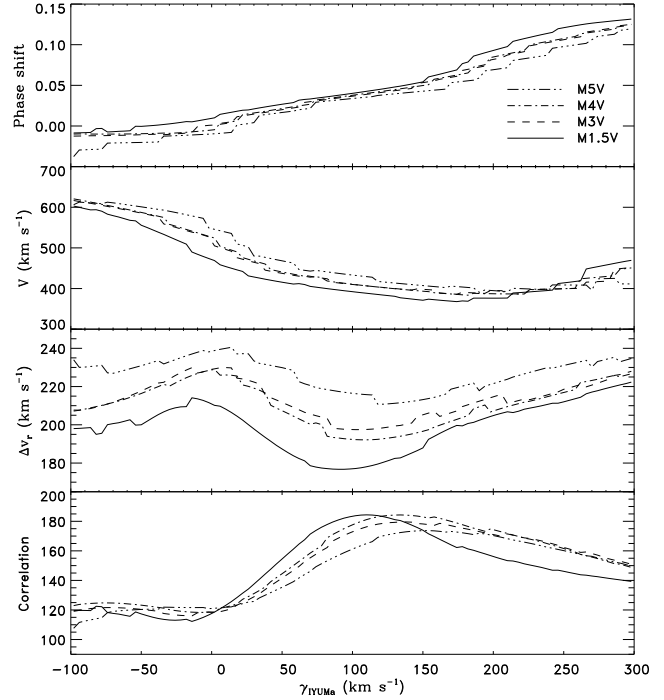


**Figure 4.** Comparison of skew maps for each template.

each image by fitting a 2-dimensional Gaussian of the form

$$C_{\vec{v}} = C_0 + C_1 \exp\left(-\frac{(v_x - v_{x,max})^2}{2\Delta v_x^2} - \frac{(v_y - v_{y,max})^2}{2\Delta v_y^2}\right)$$

where  $C_{\vec{v}}$  is the value of the skew map at velocity  $(v_x, v_y)$ . Figure 4 shows the variation in position and shape of the skew map peak as a function of  $\gamma_{\text{IYUMa}}$ . The phase shift is the angular offset of the peak from  $v_x=0$  measured about the centre of mass, i.e.  $\frac{1}{2\pi} \arctan \frac{v_{x,max}}{v_{y,max}}$ . The velocity amplitude is  $V = \sqrt{v_{x,max}^2 + v_{y,max}^2}$ . The peak width is measured using  $\Delta v_r = \sqrt{\Delta v_x^2 + \Delta v_y^2}$ . The correlation of the peak is taken as  $C_0 + C_1$ .

As  $\gamma_{\text{IYUMa}}$  increases from  $-100 \text{ km s}^{-1}$  to  $300 \text{ km s}^{-1}$ , the peak moves from a velocity of about  $600 \text{ km s}^{-1}$  and phase shift of around  $-0.01$  through the expected donor location to a lower velocity around  $400\text{--}450 \text{ km s}^{-1}$  and phase shift of around  $0.13$ . This result is true for for all four templates. Only the peak size  $\Delta v_r$  and the peak correlation vary appreciably depending on the template used. The difference in  $\Delta v_r$  between templates should not be taken as a measure of how tightly each template constrains the location of the donor: it is more likely to result from differing seeing between the different template observations. However, the variation of  $\Delta v_r$  with  $\gamma_{\text{IYUMa}}$  for each template is more useful, telling us which value of the IY UMa systemic velocity gives us the sharpest peak, and is therefore the most likely value for the systemic velocity. This shows the peak to be narrowest for  $\gamma_{\text{IYUMa}}$  around  $75$  to  $125 \text{ km s}^{-1}$ . The most important measure of which value of  $\gamma_{\text{IYUMa}}$  is correct is that for which the peak correlation is strongest. This is around  $\gamma_{\text{IYUMa}}=100$  to  $150 \text{ km s}^{-1}$  for the four templates. The peak correlation of the templates is similar, which considering the low signal-noise and resolution of these observations is not

surprising: detailed differences in the Na I doublet between the spectral types have not been resolved.

The value of  $\gamma_{\text{IYUMa}}$  with the highest peak correlation gives us one measure of the best fitting skew map. The corresponding M4V skew map is shown in the left panel of Figure 3. The average phase shift for all four of these maps is 0.044, with a spread in values of 0.001. The 360 second exposure time used corresponds to a phase resolution of 0.06, so this phase shift is consistent with the peak actually lying along the line of centres of the two stars, where we expect the donor. The accumulated error in the P2000 ephemeris at the time of these observations is only 0.005 orbits. This then gives us a donor velocity of  $K_2=383 \text{ km s}^{-1}$  with a spread of values of  $6 \text{ km s}^{-1}$ . If this measured phase shift is real, then we should also consider values of  $\gamma_{\text{IYUMa}}$  for which the phase shift is zero, placing the donor along the line of centres. The corresponding skew maps (shown for M4V in the right panel of Figure 3) give  $K_2=524 \text{ km s}^{-1}$  with a spread of  $19 \text{ km s}^{-1}$ . A possible cause of such a phase shift would be irradiation of the donor by emission from the stream-disc impact, filling-in the Na absorption mainly on the leading side of the donor, thus moving the correlation peak in the direction seen.

As described earlier, these skew maps were produced omitting phase range 0.42–0.58. As a check, the analysis was repeated using the entire phase range. The skew maps corresponding to phase shift zero show far less distinct peaks than in Figure 3, rendering this measurement less reliable. The peak in correlation, the minimum value of  $\Delta v_r$  and phase shift of zero occur for values of  $\gamma_{\text{IYUMa}}$  about 10–20  $\text{km s}^{-1}$  greater than before. The phase shift at maximum correlation is now 0.057 with a spread of 0.003, as large as the phase resolution of the data. The orbital velocity of the donor for maximum correlation is now  $K_2=362 \text{ km s}^{-1}$  with a spread of  $1 \text{ km s}^{-1}$ .

## 5 CONCLUSIONS

The donor star has been unambiguously detected in IY UMa. It is a late type M dwarf, but the low signal-to-noise and resolution of these observations prevents an accurate determination of the spectral type. The donor velocity,  $K_2$ , lies in the range about 380–540  $\text{km s}^{-1}$ , consistent with the value of 442  $\text{km s}^{-1}$  using the model-dependent orbital parameters estimated from the photometric study in P2000. Observations with a larger telescope, providing higher spectral and temporal resolution and signal-to-noise would facilitate a direct and accurate determination of both the spectral type and velocity of the donor star in IY UMa.

## 6 ACKNOWLEDGEMENTS

The data presented here have been taken using ALFOSC, which is owned by the Instituto de Astrofísica de Andalucía (IAA) and operated at the Nordic Optical Telescope under agreement between IAA and the NBIfAFG of the Astronomical Observatory of Copenhagen. The Nordic Optical Telescope is operated on the island of La Palma jointly by Denmark, Finland, Iceland, Norway, and Sweden, in the Spanish Observatorio del Roque de los Muchachos of the Instituto

de Astrofísica de Canarias. DJR would like to thank Tom Marsh for the use of his MOLLY software, and Ulrich Kolb and Brian Warner for useful comments. DJR was supported by a PPARC studentship and the OU research committee. CAH gratefully acknowledges support from the Leverhulme Trust F/00-180/A.

## REFERENCES

- Evans D.S., 1967, in Proceedings from IAU Symposium 30, eds. A.H. Batten & J. F. Heard, p.57
- Friend M.T., Martin J.S., Smith R.C., Jones D.H.P., 1988, MNRAS, 233, 451
- Friend M.T., Martin J.S., Smith R.C., Jones D.H.P., 1990a, MNRAS, 246, 637
- Friend M.T., Martin J.S., Smith R.C., Jones D.H.P., 1990b, MNRAS, 246, 654
- Hessman F.V., Robinson E.L., Nather R.E., Zhang E.H., 1984, ApJ, 286, 747
- Kirkpatrick J.D., McGraw J.T., Hess T.R., Liebert J., McCarthy D.W., 1994, ApJS, 94, 749
- Littlefair S.P., Dhillon V.S., Howell S.B., Ciardi D.R., 2000, MNRAS, 313, 117
- Marsh T.R., 1990, ApJ, 357, 621
- Patterson J., 1998, PASP, 110, 1132
- Patterson J., Kemp J., Jensen L., Vanmunster T., Skillman D.R., Martin B., Fried R., Thorstensen J.R., 2000, PASP, 112, 1567 (P2000)
- Rolfe D.J., Haswell C.A., Patterson J., 2001, MNRAS, 324, 529
- Rolfe D.J., Abbott T.M.C., Haswell C.A., 2001, in Boffin H., Steeghs D., eds, Proc. Astro-Tomography Workshop, Springer-Verlag Lecture Notes in Physics
- Rolfe D.J., Abbott T.M.C., Haswell C.A., 2002, in Gänsicke B., Beuermann K., Reinsch K., eds, Proc. The Physics of Cataclysmic Variables and Related Objects, ASP conference series
- Rolfe D.J. et al., 2002, in preparation
- Smith D., Dhillon V.S., 1998, MNRAS, 301, 767
- Smith D.A., Dhillon V.S., Marsh T.R., 1998, MNRAS, 296, 465
- Smith R.C., Collier Cameron A., Tucknott D.S., 1993, in O.Regev G.Shaviv, ed, Cataclysmic Variables and Related Objects, Inst. Phys. Publ., p.70
- Stanishev V., Kraicheva Z., Boffin H.M.J., Genkov V., 2001, A&A, 367, 273
- Ugoren A.R., 1962, AJ, 67, 37
- Wade R.A., Horne K., 1988, ApJ, 324, 411
- Wu X., Li Z., Gao W., Leung K-C., 2001, ApJ, 549, L84
- Zakhozaj V.A., 1979, Vestnik Khar'kovskogo Universiteta, 190, 52